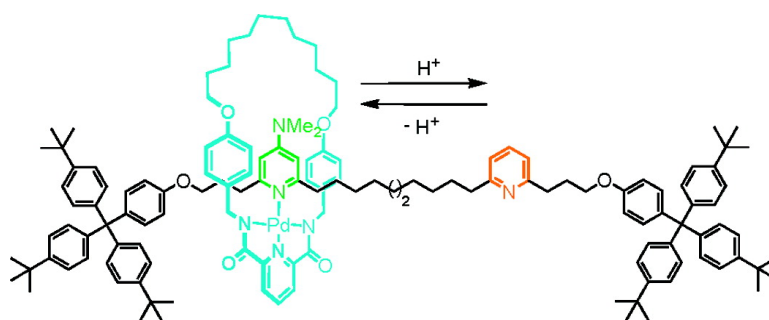


## A Switchable Palladium-Complexed Molecular Shuttle and Its Metastable Positional Isomers

James D. Crowley, David A. Leigh, Paul J. Lusby, Roy T. McBurney, Laure-Emmanuelle Perret-Aebi, Christiane Petzold, Alexandra M. Z. Slawin, and Mark D. Symes

*J. Am. Chem. Soc.*, **2007**, 129 (48), 15085-15090 • DOI: 10.1021/ja076570h

Downloaded from <http://pubs.acs.org> on February 9, 2009



### More About This Article

Additional resources and features associated with this article are available within the HTML version:

- Supporting Information
- Links to the 14 articles that cite this article, as of the time of this article download
- Access to high resolution figures
- Links to articles and content related to this article
- Copyright permission to reproduce figures and/or text from this article

[View the Full Text HTML](#)



## A Switchable Palladium-Complexed Molecular Shuttle and Its Metastable Positional Isomers

James D. Crowley,<sup>†</sup> David A. Leigh,<sup>\*,†</sup> Paul J. Lusby,<sup>†</sup> Roy T. McBurney,<sup>†</sup> Laure-Emmanuelle Perret-Aebi,<sup>†</sup> Christiane Petzold,<sup>†</sup> Alexandra M. Z. Slawin,<sup>‡</sup> and Mark D. Symes<sup>†</sup>

Contribution from the School of Chemistry, University of Edinburgh, The King's Buildings, West Mains Road, Edinburgh EH9 3JJ, United Kingdom, and the School of Chemistry, University of St. Andrews, Purdie Building, St. Andrews, Fife KY16 9ST, United Kingdom

Received August 31, 2007; E-mail: David.Leigh@ed.ac.uk

**Abstract:** We report the design, synthesis, characterization, and operation of a [2]rotaxane in which a palladium-complexed macrocycle can be translocated between 4-dimethylaminopyridine and pyridine monodentate ligand sites via reversible protonation, the metal remaining coordinated to the macrocycle throughout. The substitution pattern of the ligands and the kinetic stability of the Pd–N bond means that changing the chemical state of the thread does not automatically cause a change in the macrocycle's position in the absence of an additional input (heat and/or coordinating solvent/anion). Accordingly, under ambient conditions any of the four sets of protonated and neutral, stable, and metastable co-conformers of the [2]rotaxane can be selected, manipulated, isolated, and characterized.

### Introduction

Despite the success and influence of the redox-responsive Cu(I)/Cu(II) catenane and rotaxane systems developed in Strasbourg,<sup>1,2</sup> there are no other examples of stimuli-switchable molecular shuttles<sup>3</sup> based on the manipulation of metal–ligand interactions between the components.<sup>4,5</sup> This lack of switchable metal coordination motifs for interlocked molecules may be set to change, however, following the recognition of the need to vary the kinetics of binding events and transportation pathways (e.g., ratcheting and escapement<sup>6</sup>) in any mechanical molecular machine more sophisticated than a switch,<sup>7</sup> and the crucial role played by metastability in the functioning of rotaxanes currently being investigated for molecular electronics.<sup>8</sup> Here we describe

a simple-to-assemble-and-operate [2]rotaxane in which a palladium-complexed macrocycle can be translocated between 4-dimethylaminopyridine (DMAP) and pyridine (Py) ligand sites via reversible protonation (the metal remaining coordinated to

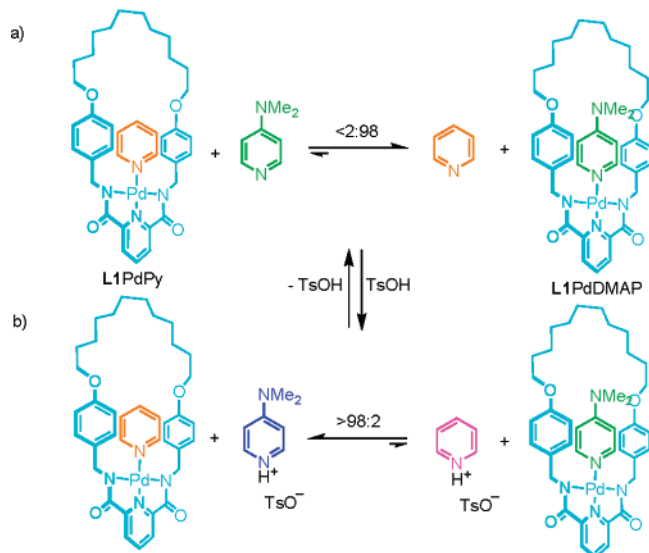
<sup>†</sup> University of Edinburgh.

<sup>‡</sup> University of St. Andrews.

- (1) For macrocycle translocation in Cu(I)/Cu(II)-coordinated rotaxanes, see: (a) Gaviña, P.; Sauvage, J.-P. *Tetrahedron Lett.* **1997**, *38*, 3521–3524. (b) Armaroli, N.; Balzani, V.; Collin, J.-P.; Gaviña, P.; Sauvage, J.-P.; Ventura, B. *J. Am. Chem. Soc.* **1999**, *121*, 4397–4408. (c) Durola, F.; Sauvage, J.-P. *Angew. Chem., Int. Ed.* **2007**, *46*, 3537–3540. For macrocycle translocation in Cu(I)/Cu(II)-coordinated catenanes, see: (d) Livoreil, A.; Dietrich-Buchecker, C. O.; Sauvage, J.-P. *J. Am. Chem. Soc.* **1994**, *116*, 9399–9400. (e) Cárdenas, D. J.; Livoreil, A.; Sauvage, J.-P. *J. Am. Chem. Soc.* **1996**, *118*, 11980–11981. (f) Livoreil, A.; Sauvage, J.-P.; Armaroli, N.; Balzani, V.; Flamigni, L.; Ventura, B. *J. Am. Chem. Soc.* **1997**, *119*, 12114–12124. For macrocycle rotation in Cu(I)/Cu(II)-coordinated rotaxanes, see: (g) Raehm, L.; Kern, J.-M.; Sauvage, J.-P. *Chem.–Eur. J.* **1999**, *5*, 3310–3317. (h) Weber, N.; Hamann, C.; Kern, J.-M.; Sauvage, J.-P. *Inorg. Chem.* **2003**, *42*, 6780–6792. (i) Poleschak, I.; Kern, J.-M.; Sauvage, J.-P. *Chem. Commun.* **2004**, 474–476. (j) Létinois-Halbes, U.; Hanss, D.; Beierle, J. M.; Collin, J.-P.; Sauvage, J.-P. *Org. Lett.* **2005**, *7*, 5753–5756. For a recent review of transition metal complexed molecular machines, see: (k) Bonnet, S.; Collin, J.-P.; Koizumi, M.; Mobian, P.; Sauvage, J.-P. *Adv. Mater.* **2006**, *18*, 1239–1250.
- (2) For contraction/stretching in a rotaxane dimer through Cu(I)–Zn(II) exchange, see: (a) Jiménez, M. C.; Dietrich-Buchecker, C.; Sauvage, J.-P. *Angew. Chem., Int. Ed.* **2000**, *39*, 3284–3287. (b) Jiménez-Molero, M. C.; Dietrich-Buchecker, C.; Sauvage, J.-P. *Chem.–Eur. J.* **2002**, *8*, 1456–1466.

- (3) (a) Bissell, R. A.; Córdova, E.; Kaifer, A. E.; Stoddart, J. F. *Nature* **1994**, *369*, 133–136. For other examples of pH-responsive molecular shuttles see: (b) Martínez-Díaz, M.-V.; Spencer, N.; Stoddart, J. F. *Angew. Chem., Int. Ed. Engl.* **1997**, *36*, 1904–1907. (c) Ashton, P. R.; Ballardini, R.; Balzani, V.; Baxter, I.; Credi, A.; Fyfe, M. C. T.; Gandolfi, M. T.; Gómez-López, M.; Martínez-Díaz, M.-V.; Piersanti, A.; Spencer, N.; Stoddart, J. F.; Venturi, M.; White, A. J. P.; Williams, D. J. *J. Am. Chem. Soc.* **1998**, *120*, 11932–11942. (d) Elizarov, A. M.; Chiu, S.-H.; Stoddart, J. F. *J. Org. Chem.* **2002**, *67*, 9175–9181. (e) Badjić, J. D.; Balzani, V.; Credi, A.; Silvi, S.; Stoddart, J. F. *Science* **2004**, *303*, 1845–1849. (f) Keaveney, C. M.; Leigh, D. A. *Angew. Chem., Int. Ed.* **2004**, *43*, 1222–1224. (g) Garaudée, S.; Silvi, S.; Venturi, M.; Credi, A.; Flood, A. H.; Stoddart, J. F. *ChemPhysChem* **2005**, *6*, 2145–2152. (h) Badjić, J. D.; Ronconi, C. M.; Stoddart, J. F.; Balzani, V.; Silvi, S.; Credi, A. *J. Am. Chem. Soc.* **2006**, *128*, 1489–1499. (i) Tokunaga, Y.; Nakamura, T.; Yoshioka, M.; Shimomura, Y. *Tetrahedron Lett.* **2006**, *47*, 5901–5904. (j) Leigh, D. A.; Thomson, A. R. *Org. Lett.* **2006**, *8*, 5377–5379.
- (4) For ruthenium-coordinated catenanes and rotaxanes which undergo photoinduced decomplexation of the components, see: (a) Mobian, P.; Kern, J.-M.; Sauvage, J.-P. *Angew. Chem., Int. Ed.* **2004**, *43*, 2392–2395. (b) Collin, J.-P.; Jouvenot, D.; Koizumi, M.; Sauvage, J.-P. *Eur. J. Inorg. Chem.* **2005**, 1850–1855. For other types of rotaxanes and catenanes which feature intercomponent metal–ligand coordination, see: (c) Hutin, M.; Schalley, C. A.; Bernardinelli, G.; Nitschke, J. R. *Chem.–Eur. J.* **2006**, *12*, 4069–4076. (d) Blight, B. A.; Wisner, J. A.; Jennings, M. C. *Chem. Commun.* **2006**, 4593–4595. (e) Blight, B. A.; Wisner, J. A.; Jennings, M. C. *Angew. Chem., Int. Ed.* **2007**, *46*, 2835–2838.
- (5) For examples of rotaxanes and catenanes which utilize transition metal ions to switch on/off other types of intercomponent interaction, see: (a) Korybut-Daszkiwicz, B.; Więckowska, A.; Bilewicz, R.; Domagała, S.; Woźniak, K. *Angew. Chem., Int. Ed.* **2004**, *43*, 1668–1672. (b) Jiang, L.; Okano, J.; Orita, A.; Otera, J. *Angew. Chem., Int. Ed.* **2004**, *43*, 2121–2124. (c) Leigh, D. A.; Lusby, P. J.; Slawin, A. M. Z.; Walker, D. B. *Angew. Chem., Int. Ed.* **2005**, *44*, 4557–4564. (d) Leigh, D. A.; Lusby, P. J.; Slawin, A. M. Z.; Walker, D. B. *Chem. Commun.* **2005**, 4919–4921. (e) Marlin, D. S.; González Cabrera, D.; Leigh, D. A.; Slawin, A. M. Z. *Angew. Chem., Int. Ed.* **2006**, *45*, 77–83. (f) Marlin, D. S.; González Cabrera, D.; Leigh, D. A.; Slawin, A. M. Z. *Angew. Chem., Int. Ed.* **2006**, *45*, 1385–1390.
- (6) Chatterjee, M. N.; Kay, E. R.; Leigh, D. A. *J. Am. Chem. Soc.* **2006**, *128*, 4058–4073.
- (7) (a) Kay, E. R.; Leigh, D. A. *Nature* **2006**, *440*, 286–287. (b) Kay, E. R.; Leigh, D. A.; Zerbetto, F. *Angew. Chem., Int. Ed.* **2007**, *46*, 72–191.

**Scheme 1.** Reversible Substitution of Pyridine and DMAP Ligands in Macrocycle–Pd Complex L1PdPy/DMAP in DMF-*d*<sub>7</sub> at 298 K<sup>a</sup>



<sup>a</sup> Upon mixing the substrates, equilibrium is reached within the time taken to acquire a <sup>1</sup>H NMR spectrum. (a) Neutral conditions; (b) in the presence of TsOH (1 equiv).

the macrocycle throughout). The substitution pattern of the ligands and the kinetic stability of the Pd–N bond means that changing the chemical state of the thread (adding or removing protons) does not automatically cause a change in the macrocycle’s position in the absence of an additional input (heat and/or coordinating solvent/anion). Accordingly, under ambient conditions any of the four sets of protonated and neutral, stable, and metastable co-conformers of the [2]rotaxane can be selected, manipulated, isolated, and characterized.

## Results and Discussion

**Basis of the Design: Protonation/Deprotonation-Driven Ligand Exchange Experiments.** The shuttle is based on a recognition motif previously used to assemble rotaxanes and catenanes by organizing tridentate pyridine 2,6-dicarboxamide and appropriately derivatized monodentate pyridine ligands about a square planar Pd(II) template.<sup>9</sup> In a simple exchange experiment with non-interlocked versions of these ligands

(Scheme 1a), we found that the pyridine group of L1PdPy was rapidly<sup>10</sup> and quantitatively substituted for DMAP.<sup>11</sup> By adding an equivalent of *p*-toluenesulfonic acid (TsOH), the process could be reversed (Scheme 1b).<sup>12</sup> The reasons for the selectivity in Scheme 1b are quite subtle: although both heterocycles are “coordinated”—one to Pd(II) and one to H<sup>+</sup>—on both sides of the equation (Scheme 1b), protonation of the more basic heterocycle determines the position of equilibrium because the N–H bond is significantly stronger than the Pd–N bond.<sup>13</sup> In other words, a proton differentiates DMAP and Py more effectively than does Pd(II). The results suggested that a palladium-complexed [2]rotaxane incorporating both DMAP and Py binding sites in the thread could operate as a pH-switchable molecular shuttle.

**Synthesis and Characterization of Palladium-Coordinated Molecular Shuttle L2Pd.** A candidate [2]rotaxane, L2Pd, was synthesized in nine steps using a “threading-followed-by-stoppering” strategy<sup>14</sup> (Scheme 2). 2,6-Diiodo-4-dimethylaminopyridine, **1**, was prepared via a modified literature procedure<sup>15</sup> (Scheme 2, step a) and subjected to consecutive Sonogashira cross-coupling reactions,<sup>16</sup> first with propargyl alcohol (1 equiv) and then with decadiyne (5 equiv), to afford the unsymmetrical DMAP-station<sup>17</sup> intermediate **3** (Scheme 2, step c). The synthesis of the Py-station fragment was achieved by desymmetrization of commercially available 2,6-dibromopyridine through a Sonogashira cross-coupling with 1 equiv of propargyl alcohol to give **2** (Scheme 2, step b), hydrogenation (over PtO<sub>2</sub>), and Mitsunobu reaction<sup>18</sup> with bulky phenol **4**<sup>19</sup> to give **5** (Scheme 2, step d). The coupling of **3** and **5** via another Pd-catalyzed Sonogashira reaction, and subsequent hydrogenation over Pd(OH)<sub>2</sub>/C, afforded the saturated monostoppered thread, **6** (Scheme 2, step e). Coordination of the macrocycle–palladium complex to the DMAP site of **6** occurred upon simple stirring with L1Pd(CH<sub>3</sub>CN)<sup>9c</sup> in dichloromethane (298 K, 1 h). The resulting threaded pseudo-rotaxane complex was covalently

- (8) (a) Tseng, H.-R.; Wu, D.; Fang, N. X.; Zhang, X.; Stoddart, J. F. *ChemPhysChem* **2004**, *5*, 111–116. (b) Steuerman, D. W.; Tseng, H.-R.; Peters, A. J.; Flood, A. H.; Jeppesen, J. O.; Nielsen, K. A.; Stoddart, J. F.; Heath, J. R. *Angew. Chem., Int. Ed.* **2004**, *43*, 6486–6491. (c) Flood, A. H.; Peters, A. J.; Vignon, S. A.; Steuerman, D. W.; Tseng, H.-R.; Kang, S.; Heath, J. R.; Stoddart, J. F. *Chem.–Eur. J.* **2004**, *10*, 6558–6564. (d) Flood, A. H.; Stoddart, J. F.; Steuerman, D. W.; Heath, J. R. *Science* **2004**, *306*, 2055–2056. (e) Choi, J. W.; Flood, A. H.; Steuerman, D. W.; Nygaard, S.; Braunschweig, A. B.; Moonen, N. N. P.; Laursen, B. W.; Luo, Y.; Delonno, E.; Peters, A. J.; Jeppesen, J. O.; Xe, K.; Stoddart, J. F.; Heath, J. R. *Chem.–Eur. J.* **2006**, *12*, 261–279.
- (9) (a) Fuller, A.-M.; Leigh, D. A.; Lusby, P. J.; Oswald, I. D. H.; Parsons, S.; Walker, D. B. *Angew. Chem., Int. Ed.* **2004**, *43*, 3914–3918. (b) Furusho, Y.; Matsuyama, T.; Takata, T.; Moriuchi, T.; Hirao, T. *Tetrahedron Lett.* **2004**, *45*, 9593–9597. (c) Fuller, A.-M. L.; Leigh, D. A.; Lusby, P. J.; Slawin, A. M. Z.; Walker, D. B. *J. Am. Chem. Soc.* **2005**, *127*, 12612–12619. (d) Leigh, D. A.; Lusby, P. J.; Slawin, A. M. Z.; Walker, D. B. *Angew. Chem., Int. Ed.* **2005**, *44*, 4557–4564. (e) Fuller, A.-M. L.; Leigh, D. A.; Lusby, P. J. *Angew. Chem., Int. Ed.* **2007**, *46*, 5015–5019.
- (10) Exchange of the unsubstituted heterocycles in CDCl<sub>3</sub>, C<sub>2</sub>D<sub>2</sub>Cl<sub>4</sub>, or DMF-*d*<sub>7</sub> was complete within the time frame of mixing the L1PdPy complex with DMAP and acquiring a <sup>1</sup>H NMR spectrum, as was the reverse proton-driven exchange upon adding TsOH. However, the 2,6-dipropyl substituted heterocycles did not exchange in CDCl<sub>3</sub> even over extended periods (7 d) or upon heating at reflux. In DMF-*d*<sub>7</sub> at 358 K equilibrium was reached after 60 min (neutral conditions) or 130 min (in the presence of TsOH). For full details of the exchange experiments, see the Supporting Information.

- (11) For the exchange of various 4-substituted pyridine ligands at the fourth coordination site of Pd–pincer complexes, see: (a) van Manen, H.-J.; Nakashima, K.; Shinkai, S.; Kooijman, H.; Spek, A. L.; van Veggel, F. C. J. M.; Reinhoudt, D. N. *Eur. J. Inorg. Chem.* **2000**, 2533–2540. The exchange of DMAP for poly(4-vinylpyridine) at the fourth coordination site of bimetallic Pd– and Pt–pincer complexes has been exploited in the chemoresponsive viscosity switching of a metallo-supramolecular network; see: (b) Loveless, D. M.; Jeon, S. L.; Craig, S. L. *J. Mater. Chem.* **2007**, *17*, 56–61.
- (12) A proton-driven ligand exchange of diethylamine and lutidine coordinated to Pd(II) has previously been reported; see: (a) Hamann, C.; Kern, J.-M.; Sauvage, J.-P. *Dalton Trans.* **2003**, 3770–3775. For the proton-driven exchange of one amine for another within copper-coordinated imine ligands, see: (b) Nitschke, J. R. *Angew. Chem., Int. Ed.* **2004**, *43*, 3073–3075. (c) Nitschke, J. R.; Schultz, D.; Bernardinelli, G.; Gérard, D. *J. Am. Chem. Soc.* **2004**, *126*, 16538–16543. (d) Schultz, D.; Nitschke, J. R. *Proc. Natl. Acad. Sci. U.S.A.* **2005**, *102*, 11191–11195. (e) Nitschke, J. R. *Acc. Chem. Res.* **2007**, *40*, 103–112.
- (13) (a) Sanderson, R. T. *Chemical Bonds & Bond Energy*; Academic Press: New York, 1976. (b) Cotton, F. A.; Wilkinson, G.; Murillo, C.; Bochmann, M.; Grimes, R.; Murillo, C. A.; Bochmann M. *Advanced Inorganic Chemistry: A Comprehensive Text*, 6th ed.; John Wiley & Sons: New York, 1999. A contributing reason as to why the proton discriminates DMAP and pyridine better than the Pd–macrocycle complex may be because the proton is charged while the Pd–macrocycle is not. However, since this is not the situation in ref 12a, where proton-driven ligand exchange at Pd(II) also occurs, it is presumably not a major factor in the present system either.
- (14) Amabilino, D. B.; Stoddart, J. F. *Chem. Rev.* **1995**, *95*, 2725–2828.
- (15) Wayman, K. A.; Sammakia, T. *Org. Lett.* **2003**, *5*, 4105–4108.
- (16) Sonogashira, K.; Tohda, Y.; Hagihara, N. *Tetrahedron Lett.* **1975**, *16*, 4467–4470.
- (17) The italicized prefixes DMAP- and Py- denote the position of the macrocycle on the thread in the rotaxane.
- (18) Mitsunobu, O.; Yamada, Y. *Bull. Chem. Soc. Jpn.* **1967**, *40*, 2380–2382.
- (19) Gibson, H. W.; Lee, S. H.; Engen, P. T.; Lecavalier, P.; Sze, J.; Shen, Y. X.; Bheda, M. *J. Org. Chem.* **1993**, *58*, 3748–3756.

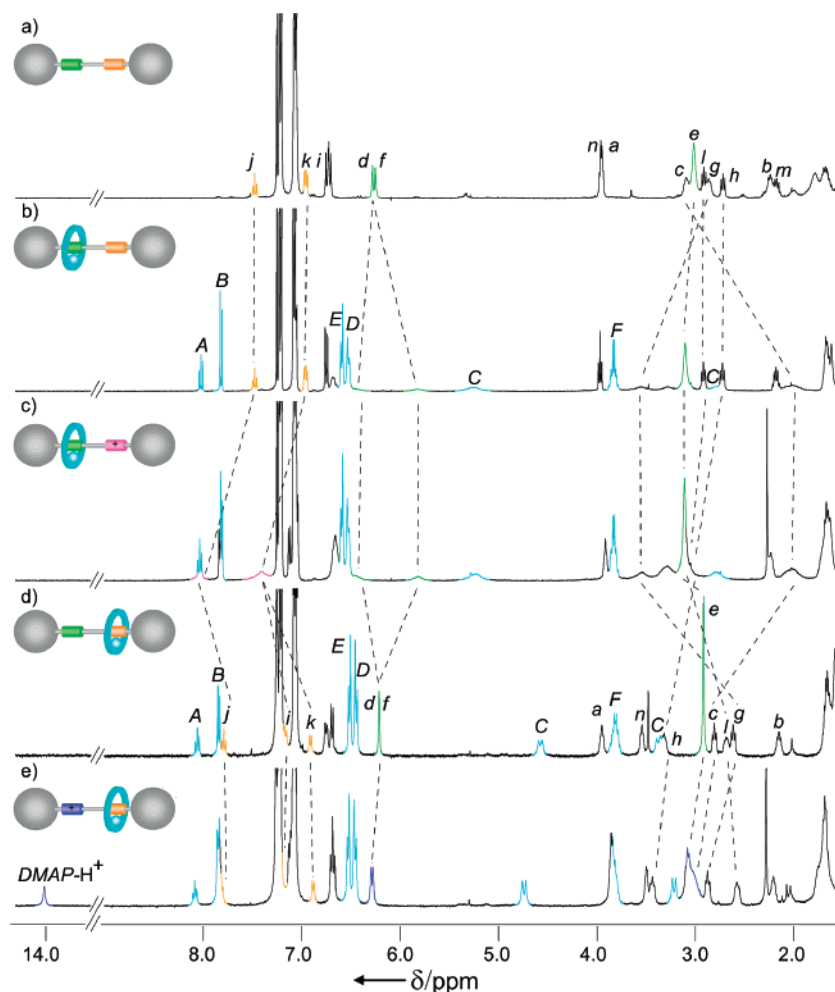


**Figure 1.**  $^1\text{H}$  NMR spectra (400 MHz,  $\text{CDCl}_3$ , 300 K) of palladium rotaxane **L2Pd** in its four different protonated and co-conformational states, and for comparison the free thread: (a) Thread **8**; (b) *DMAP*-**L2Pd**; (c) *DMAP*-[**L2HPd**]OTs; (d) *Py*-**L2Pd**; (e) *Py*-[**L2HPd**]OTs. The lettering in the figure refers to the assignments in Scheme 2.

captured with **4** (DIAD,  $\text{PPh}_3$ , THF) to give the [2]rotaxane, **L2Pd**, in 26% yield<sup>20</sup> after column chromatography (Scheme 2, step f).

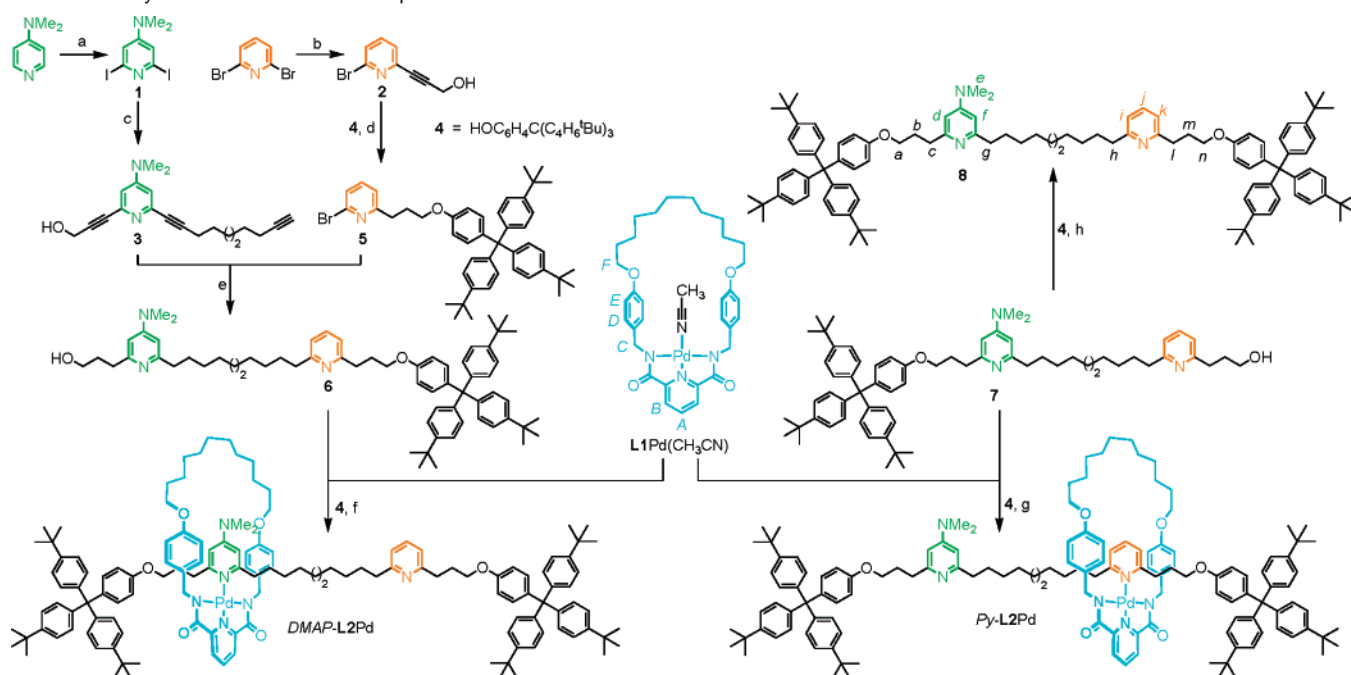
Mass spectrometry confirmed the product's constitution as **L2Pd**, and  $^1\text{H}$  NMR spectroscopy (Figure 1b) showed the co-conformation formed to be exclusively *DMAP*-**L2Pd**;<sup>17</sup> i.e., the Pd-macrocycle fragment, **L1Pd**, was solely coordinated to the *DMAP* binding site. A comparison of the spectra of free thread **8** (Figure 1a) and *DMAP*-**L2Pd** in  $\text{CDCl}_3$  (Figure 1b) shows significant differences between the signals of the *DMAP* station ( $\text{H}_{d-f}$ ) for the rotaxane and thread, while the *Py* station signals ( $\text{H}_{i-k}$ ) of the rotaxane occur at very similar values to those of the free thread. Interestingly, and for reasons that would become apparent later, attempting the threading protocol with **7**, a close analogue of **6** in which the positions of the two stations were reversed (i.e., the *Py* binding site was closest to the unstoppered end of the thread; Scheme 2, step g), led exclusively to the formation of *Py*-**L2Pd**! The outcomes of the two threading reactions indicate that the pyridine and *DMAP* binding sites are both astonishingly efficient at capturing the Pd-macrocycle component from **L1Pd**( $\text{CH}_3\text{CN}$ ) on its initial pass over the

heterocycle at the open end of the thread, irrespective of relative orientation, solvation, or other factors.

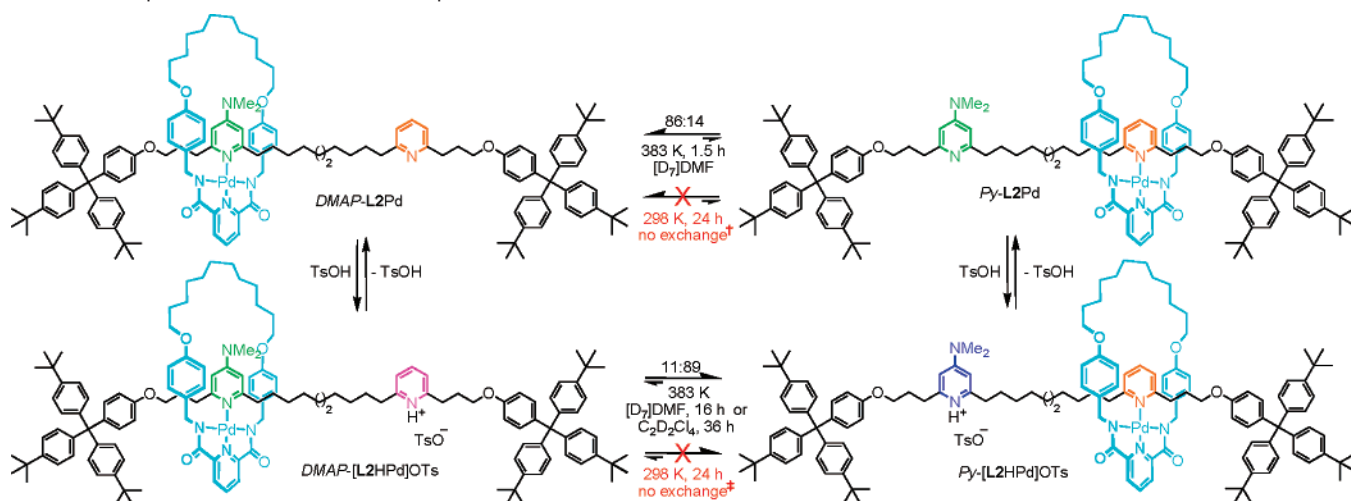
**Macrocycle-to-Py-Station Protonation-Driven Shuttling Experiments.** Switching of the macrocycle position in *DMAP*-**L2Pd** was attempted by the addition of 1 equiv of TsOH in  $\text{CDCl}_3$  (Scheme 3). The  $^1\text{H}$  NMR spectrum of the resulting adduct (Figure 1c) showed significant changes in the *Py* resonances,  $\text{H}_{i-k}$ , but no discernible shift of the *DMAP* signals,  $\text{H}_{d-f}$ , indicating that protonation of the *Py* station had occurred but the position of the macrocycle had not changed; i.e., the chemical structure was now *DMAP*-[**L2HPd**]OTs (Scheme 3). No changes to the  $^1\text{H}$  NMR spectrum of the sample were observed over several days, indicating that the co-conformer is effectively stable at room temperature in  $\text{CDCl}_3$ . Somewhat surprisingly, however, given the results of the exchange experiments reported in Scheme 1,<sup>10</sup> even in neat coordinating solvents ( $\text{DMSO}-d_6$  or  $\text{DMF}-d_7$ ) no evidence of translocation of the ring in *DMAP*-[**L2HPd**]OTs was observed at room temperature. Translocation of the palladium macrocycle sub-component (**L1Pd**) only takes place at elevated temperatures (383 K), in both coordinating ( $\text{DMF}-d_7$ ) and non-coordinating solvents ( $\text{C}_2\text{D}_2\text{Cl}_4$ ), in both cases reaching an equilibrium 89:11 ratio of *Py*:*DMAP*-[**L2HPd**]OTs (Scheme 3) after 16 h ( $\text{DMF}-d_7$ ) or 36 h ( $\text{C}_2\text{D}_2\text{Cl}_4$ ).

(20) The modest yield of rotaxane in the stoppering step is probably a consequence of using a triphenylphosphine-mediated reaction with a Pd-complexed pseudo-rotaxane. Alternative methodologies are currently being investigated.



**Scheme 2.** Synthesis of Palladium-Complexed Molecular Shuttle **L2Pd**<sup>a</sup>

<sup>a</sup> Reagents and conditions: (a)  $\text{BF}_3 \cdot \text{OEt}_2$ , LDA,  $\text{I}_2$ , THF, 40%; (b) propargyl alcohol,  $\text{Pd}(\text{PPh}_3)_4$ , CuI,  $\text{Et}_3\text{N}/\text{THF}$  (1:2), 60%; (c) (i) propargyl alcohol,  $\text{Pd}(\text{PPh}_3)_4$ , CuI,  $\text{Et}_3\text{N}/\text{THF}$ , 75%, (ii) 1,9-decadiyne (5 equiv),  $\text{Pd}(\text{PPh}_3)_4$ , CuI,  $\text{Et}_3\text{N}/\text{THF}$ , 77%; (d) (i)  $\text{H}_2$ ,  $\text{PtO}_2$ ,  $\text{EtOH}/\text{Et}_3\text{N}$ , 94%, (ii) **4**, DIAD,  $\text{PPh}_3$ , THF, 61%; (e) (i)  $\text{Pd}(\text{PPh}_3)_4$ , CuI,  $\text{Et}_3\text{N}/\text{THF}$ , 66%, (ii)  $\text{H}_2$ ,  $\text{Pd}(\text{OH})_2/\text{C}$ , THF, 88%; (f) (i) **L1Pd**( $\text{CH}_3\text{CN}$ ),  $\text{CH}_2\text{Cl}_2$  (90%), (ii) **4**, DIAD,  $\text{PPh}_3$ , THF, 26% (from **6**); (g) (i) **L1Pd**( $\text{CH}_3\text{CN}$ ),  $\text{CH}_2\text{Cl}_2$  (67%), (ii) **4**, DIAD,  $\text{PPh}_3$ , THF, 21% (from **7**); (h) **4**, DIAD,  $\text{PPh}_3$ , THF, 25%.

**Scheme 3.** Operation of the Palladium-Complexed Molecular Shuttle **L2Pd**<sup>a</sup>

<sup>a</sup> † No macrocycle translocation observed over 24 h in  $\text{DMF-}d_7$  at 298 K or in  $\text{C}_2\text{D}_2\text{Cl}_4$  over 24 h at 383 K; ‡ No macrocycle translocation observed in either  $\text{DMF-}d_7$  or  $\text{C}_2\text{D}_2\text{Cl}_4$  at 298 K over 24 h.

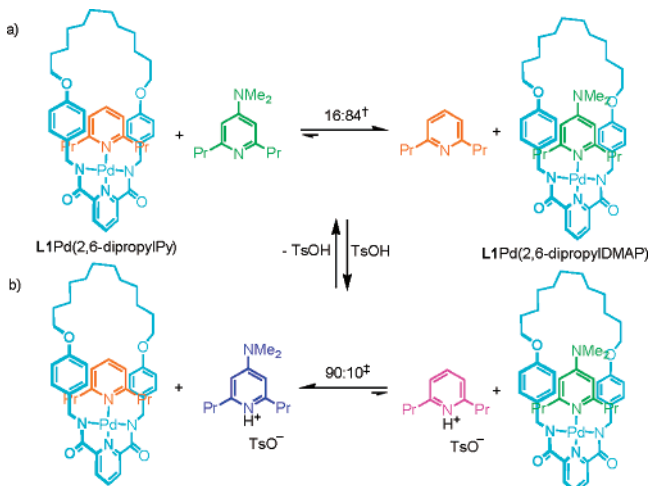
**Ligand Exchange Experiments and X-ray Crystallography Using 2,6-Dialkyl-Substituted Heterocycles.** The dramatic kinetic stability of the *DMAP*–Pd bond in the protonated [2]rotaxane led us to re-examine the kinetics of non-interlocked ligand exchange, this time using 2,6-dialkyl-substituted heterocycles (Scheme 4). Indeed, using 2,6-dipropylpy and 2,6-dipropylDMAP as the monodentate components of the **L1Pd**–heterocycle complex (Scheme 4) produced the same extremely slow exchange of ligands observed in the [2]rotaxane. Single crystals of both **L1Pd**(2,6-dipropylpy) and **L1Pd**(2,6-dipropylDMAP) were subsequently grown by vapor diffusion of diethyl ether into saturated solutions of the complexes in dichloromethane. The X-ray crystal structures of these two complexes (Figure 2a and 2b) are indicative of the likely coordination mode

and geometry of the macrocycle at the two different binding sites in the [2]rotaxane. The crystal structures suggest that the reason for the enhanced kinetic stability of the Pd-coordinated 2,6-dialkylheterocycle units is that the  $\alpha$ -hydrogen atoms of the alkyl substituents block the pathway of incoming nucleophiles to the Pd center.<sup>21</sup>

**Macrocycle-to-DMAP-Station Deprotonation-Driven Shutling Experiments.** Deprotonation of the 89:11 *Py*:*DMAP* equilibrium mixture of [**L2HPd**]OTs ( $\text{Na}_2\text{CO}_3$ ,  $\text{CH}_2\text{Cl}_2$ , 30 min) generated the neutral co-conformers which were readily sepa-

(21) Similar effects have been observed upon increasing the steric bulk about the coordination sphere in other Pd and Pt complexes. For examples, see: (a) Atwood, J. D. *Inorganic and Organometallic Reaction Mechanisms*, 2nd ed.; Wiley-VCH: New York, 1997. (b) Yount, W. C.; Loveless, D. M.; Craig, S. L. *J. Am. Chem. Soc.* **2005**, *127*, 14488–14496.

**Scheme 4.** Reversible Substitution of 2,6-Dipropylpyridine and 2,6-DipropylDMAP Ligands in Macrocycle–Pd Complex  $L1Pd(2,6\text{-dipropylPy})/(2,6\text{-dipropylDMAP})$  in  $DMF-d_7^a$



<sup>a</sup> (a) Neutral conditions; (b) in the presence of TsOH (1 equiv). Time required to reach equilibrium: <sup>†</sup> 60 min at 358 K; <sup>‡</sup> 130 min at 358 K. No exchange of the 2,6-dipropylheterocycle ligands was observed in  $CDCl_3$ , under either neutral conditions or in the presence of TsOH, even under heating at reflux over 7 d.

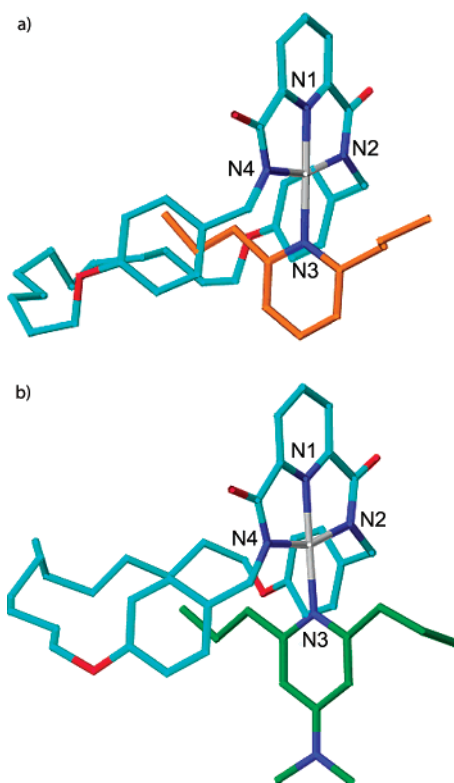


**Figure 2.** X-ray crystal structures of (a)  $L1Pd(2,6\text{-dipropylPy})$  and (b)  $L1Pd(2,6\text{-dipropylDMAP})$ . Carbon atoms of the macrocycle are shown in light blue, and those of the monodentate ligands, in orange and green, respectively; oxygen atoms are red; nitrogen, dark blue; and palladium, gray. Selected bond lengths [Å] and angles [deg]: (a) N1–Pd 1.94, N2–Pd 2.03, N3–Pd 2.06, N4–Pd 2.03, N2–Pd–N4 161.6; (b) N1–Pd 1.93, N2–Pd 2.03, N3–Pd 2.06, N4–Pd 2.02, N2–Pd–N4 161.4.

rated by column chromatography to give pure, kinetically stable samples of both  $DMAP\text{-}L2Pd$  (minor product) and  $Py\text{-}L2Pd$  (major product). Their  $^1H$  NMR spectra are shown in Figure 1b and 1d, respectively. As before, the relative shifts of the resonances of the  $DMAP$  and  $Py$  stations unambiguously

confirmed the position of the macrocycle in the  $Py\text{-}L2Pd$  isomer. Reprotonation of  $Py\text{-}L2Pd$  (1 equiv of TsOH in  $CDCl_3$ ) quantitatively generated  $Py\text{-}[L2HPd]OTs$  ( $^1H$  NMR spectrum, Figure 1e), as another kinetically stable, out-of-equilibrium conformer.

To complete the cycle of operations on  $L2Pd$ , pure  $Py\text{-}L2Pd$  and the nonequilibrium, 11:89, mixture of  $DMAP/Py\text{-}L2Pd$  were each heated at 383 K in  $DMF-d_7$ . After 90 min both had reached identical 86:14 ratios of  $DMAP/Py\text{-}L2Pd$  which did not change upon further heating (Scheme 3). Unlike the proton-driven translocation, no macrocycle translational isomerization was observed when  $Py\text{-}L2Pd$  was heated in  $C_2D_2Cl_4$ . Similarly, 2,6-dipropylDMAP did not undergo a substitution reaction with  $L1Pd(2,6\text{-dipropylPy})$  in non-coordinating solvents (Scheme 4).

## Conclusions

The practical realization and mechanistic investigation of molecular-level systems in which both the kinetics and thermodynamics of binding events can be varied and controlled is profoundly important for the development of sophisticated molecular machine systems.<sup>7b</sup> Although nature is clearly able to achieve this through the rapid manipulation of hydrogen bonding and electrostatic interactions, the transient nature of such weak binding events makes it hard to see how to emulate this in synthetic systems given current levels of understanding and expertise. We anticipate that metal–ligand coordination (and dynamic covalent chemistry) will play a prominent role in the early development of synthetic molecular machine systems.

## Experimental Section

**Synthesis of  $DMAP\text{-}L2Pd$  from **6** and Selected Spectroscopic Data:** To a solution of **6** (0.043 g, 0.046 mmol, 1.0 equiv) in  $CH_2Cl_2$  (30 mL) was added  $L1Pd(CH_3CN)$  (0.032 g, 0.046 mmol, 1.0 equiv), and the solution stirred at RT for 1 h. The solvent was removed under reduced pressure, and the crude residue was purified by column chromatography ( $MeOH/CH_2Cl_2$ , 4:96) to give the threaded pseudo-rotaxane (0.066 g, 90%). To a solution of the pseudo-rotaxane (0.054 g, 0.0304 mmol, 1.0 equiv),  $PPh_3$  (0.013 g, 0.0509 mmol, 1.5 equiv), and **4** (0.026 g, 0.0509 mmol, 1.5 equiv) in THF (10 mL) was added DIAD (0.010 mL, 0.0509 mmol, 1.5 equiv) *via* microsyringe, and the resulting solution was stirred at RT for 36 h. After removal of the solvent under reduced pressure, the crude residue was purified by column chromatography on silica ( $EtOAc:CH_2Cl_2$  2:3) and washed with ice-cold  $CH_3CN$  to yield  $DMAP\text{-}L2Pd$  as a yellow solid (0.025 g, yield = 29% from the pre-rotaxane, 26% from **6**). Mp 170–172 °C;  $^1H$  NMR (400 MHz,  $CDCl_3$ ):  $\delta$  = 1.01–1.43 (m, 84H, *Bu-Stopper-H* + *thread-alkyl-H* + *macrocycle-alkyl-H* +  $H_b$ ), 1.61–1.79 (m, 6H, *thread-alkyl-H* + *macrocycle-alkyl-H*), 2.01 (br, 4H, *thread-alkyl-H* +  $H_c$ ), 2.15–2.25 (m, 2H,  $H_m$ ), 2.65–3.38 (m, 14H,  $H_{a++b++c}$ ), 3.55 (br, 2H,  $H_g$ ), 3.80–3.89 (m, 4H,  $H_f$ ), 3.98 (t,  $J$  = 6.3, 2H,  $H_n$ ), 5.25 (br, 2H,  $H_c$ ), 5.82 (br, 1H,  $H_j$ ), 6.40–6.80 (m, 13H, *stopper-H* +  $H_{D+E+d}$ ), 6.93–7.02 (m, 2H,  $H_{+k}$ ), 7.05–7.11 (m, 16H, *stopper-H*), 7.19–7.25 (m, 12H, *stopper-H*), 7.45–7.53 (m, 1H,  $H_j$ ), 7.83 (d,  $J$  = 7.8, 2H,  $H_B$ ), 8.04 (t,  $J$  = 7.8, 1H,  $H_A$ ); LRESI-MS ( $MeOH/CH_2Cl_2/TFA$ ):  $m/z$  = 2075 [ $M^+$ ]; HR-FABMS (3-NOBA matrix):  $m/z$  = 2075.20724 [ $M^+$ ] (calcd for  $C_{135}H_{168}N_6O_6^{106}Pd$ , 2075.20601).

**Preparation of  $DMAP\text{-}[L2HPd]OTs$ :** To a solution of  $DMAP\text{-}L2Pd$  (0.0295 g, 0.0142 mmol, 1.0 equiv) in  $CDCl_3$  (2 mL) was added TsOH (0.00270 g, 0.0142 mmol, 1.0 equiv), and the reaction stirred at RT until all the TsOH had dissolved (5 min).  $^1H$  NMR spectroscopy revealed quantitative formation of  $DMAP\text{-}[L2HPd]OTs$ .  $^1H$  NMR (400 MHz,  $CDCl_3$ ):  $\delta$  = 1.00–1.40 (m, 82H, *stopper-H* + *alkyl-thread-H* + *alkyl-macrocycle-H*), 1.59–1.77 (m, 10H, *thread-alkyl-H* +  $H_b$ ), 2.03

(br, 2H, H<sub>c</sub>), 2.19–2.31 (m, 5H, *tosyl*-H + H<sub>m</sub>), 2.69–3.42 (m, 14H, H<sub>a+e+h+i+c</sub>), 3.56 (br, 2H, H<sub>g</sub>), 3.79–3.94 (m, 6H, H<sub>n+f</sub>), 5.23 (br, 2H, H<sub>c</sub>), 5.82 (br, 1H, H<sub>j</sub>), 6.39–6.71 (m, 13H, *stopper*-H + H<sub>d+d+e</sub>), 7.05–7.14 (m, 18H, *stopper*-H + *tosyl*-H), 7.21–7.24 (m, 12H, *stopper*-H), 7.44 (br, 2H, H<sub>i+k</sub>), 7.82–7.85 (m, 4H, *tosyl*-H + H<sub>B</sub>), 8.02–8.14 (m, 2H, H<sub>j+A</sub>).

**Preparation of Py-L2Pd via the Protonation-Driven Translational Isomerization and Subsequent Deprotonation of DMAP-[L2HPd]-OTs:** DMAP-[L2HPd]OTs (0.0322 g, 0.0142 mmol) was dissolved in DMF-*d*<sub>7</sub> (1 g), and a control <sup>1</sup>H NMR spectrum acquired before the sample was heated at 383 K. The sample was monitored regularly by <sup>1</sup>H NMR spectroscopy. An equilibrium ratio of 89:11 *Py*:DMAP-[L2HPd]OTs was reached after 16 h and remained unchanged upon further heating. (Similarly, heating DMAP-[L2HPd]OTs at 383 K in C<sub>2</sub>D<sub>2</sub>Cl<sub>4</sub> for 36 h gave the same ratio of isomers, and subsequent heating did not alter the product distribution.) After removal of DMF-*d*<sub>7</sub> under reduced pressure, the reaction mixture was redissolved in CH<sub>2</sub>Cl<sub>2</sub> (10 mL) and stirred with a large excess of Na<sub>2</sub>CO<sub>3</sub> (5 g) for 30 min. Filtration through celite followed by removal of the solvent under reduced pressure gave a yellow solid. <sup>1</sup>H NMR (400 MHz, CDCl<sub>3</sub>) analysis revealed that the crude residue was comprised of a mixture of *Py*:DMAP-L2Pd in an (unchanged) 89:11 ratio. The two co-conformers were separated by column chromatography on silica gel (MeOH/CH<sub>2</sub>-Cl<sub>2</sub> 1:19) to give pure samples of both DMAP-L2Pd (identical spectroscopic and other physical data to the sample previously obtained) and *Py*-L2Pd. <sup>1</sup>H NMR (400 MHz, CDCl<sub>3</sub>): δ = 1.07–1.43 (m, 82H, *stopper*-H + *thread*-alkyl-H + *macrocycle*-alkyl-H), 1.47–1.72 (m, 10H, *thread* alkyl-H + *macrocycle*-alkyl-H + H<sub>g</sub>), 2.14–2.23 (m, 2H, H<sub>b</sub>), 2.57–3.00 (m, 12H, H<sub>c+e+g+i</sub>), 3.29–3.43 (m, 4H, H<sub>h+c</sub>), 3.52–3.59 (m, 2H, H<sub>n</sub>), 3.78–3.88 (m, 4H, H<sub>f</sub>), 3.93–4.00 (m, 2H, H<sub>d</sub>), 4.59 (d, *J* = 12.5, 2H, H<sub>c</sub>), 6.21–6.23 (m, 2H, H<sub>d+j</sub>), 6.44–6.47 (m, 4H, H<sub>D</sub>), 6.49–6.56 (m, 4H, H<sub>E</sub>), 6.68–6.79 (m, 4H, *stopper*-H), 6.92 (d, *J* = 7.6, 1H, H<sub>k</sub>), 7.05–7.11 (m, 16H, *stopper*-H), 7.17–7.24 (m, 13H, *stopper*-H + H<sub>h</sub>), 7.79–7.82 (m, 1H, H<sub>j</sub>), 7.84–7.87 (m, 2H, H<sub>B</sub>), 8.05–8.09 (m, 1H, H<sub>A</sub>).

**Preparation of Pure Py-[L2HPd]OTs:** To a solution of *Py*-L2Pd (0.0221 g, 0.0106 mmol, 1.0 equiv) in CDCl<sub>3</sub> (2 mL) was added TsOH (0.00202 g, 0.0106 mmol, 1.0 equiv), and the reaction stirred at RT until all the TsOH had dissolved (5 min). <sup>1</sup>H NMR spectroscopy revealed quantitative formation of *Py*-[L2HPd]OTs. <sup>1</sup>H NMR (400 MHz, CDCl<sub>3</sub>): δ = 1.47–1.66 (m, 82H, *stopper*-H + *thread*-alkyl-H + *macrocycle*-alkyl-H), 1.58–1.81 (m, 10H, *thread*-alkyl-H + *macrocycle*-alkyl-H + H<sub>m</sub>), 2.16–2.32 (m, 5H, *tosyl*-H + H<sub>b</sub>), 2.53–2.63 (m, 2H, H<sub>i</sub>), 2.83–3.26 (m, 12H, H<sub>c+e+g+c</sub>), 3.40–3.53 (m, 4H, H<sub>n+n</sub>), 3.79–3.90 (m, 6H, H<sub>a+f</sub>), 4.74 (d, *J* = 13.9, 2H, H<sub>c</sub>), 6.28 (d, *J* = 7.6, 2H, H<sub>d+j</sub>), 6.42–6.57 (m, 8H, H<sub>D+E</sub>), 6.66–6.71 (m, 4H, *stopper*-H), 6.88 (d, *J* = 7.3, 1H, H<sub>k</sub>), 7.02–7.15 (m, 19H, *stopper*-H + *tosyl*-H + H<sub>j</sub>), 7.18–7.26 (m, 12H, *stopper*-H), 7.80–7.86 (m, 5H, *tosyl*-H + H<sub>j+B</sub>), 8.06–8.10 (m, 1H, H<sub>A</sub>), 14.00 (br, 1H, DMAP-H).

**Preparation of DMAP-L2Pd via Translational Isomerization of Py-L2Pd:** Rotaxane *Py*-L2Pd was heated to 110 °C in DMF-*d*<sub>7</sub> (1 g)

and monitored *via* <sup>1</sup>H NMR spectroscopy at regular intervals. A ratio of 86:14 DMAP:*Py*-L2Pd was established after 1.5 h, and further heating did not alter this ratio. Upon heating pure *Py*-L2Pd to 110 °C in C<sub>2</sub>D<sub>2</sub>-Cl<sub>4</sub>, no isomerization was observed, even after 7 days of heating at 383 K.

**X-ray Crystallographic Structure Determinations.** Single crystals of L1Pd(2,6-dipropylPy) and L1Pd(2,6-dipropylDMAP) of suitable quality for X-ray diffraction studies were grown by the vapor diffusion of Et<sub>2</sub>O into CH<sub>2</sub>Cl<sub>2</sub> solutions of the complexes. Structural data for both L1Pd(2,6-dipropylPy) and L1Pd(2,6-dipropylDMAP) were collected at 93 K using a Rigaku Mercury diffractometer (MM007 high-flux RA/Mo Kα radiation, confocal optic). All data collections employed narrow frames (0.3–1.0) to obtain at least a full hemisphere of data. Intensities were corrected for Lorentz polarization and absorption effects (multiple equivalent reflections). The structures were solved by direct methods, and non-hydrogen atoms were refined anisotropically with CH protons being refined in riding geometries (SHELXTL) against *F*<sup>2</sup>. L1Pd(2,6-dipropylDMAP): C<sub>46</sub>H<sub>61</sub>N<sub>5</sub>O<sub>4</sub>Pd, *M<sub>r</sub>* = 854.40, yellow prism, crystal size = 0.08 × 0.08 × 0.08 mm<sup>3</sup>, monoclinic, *P*<sub>2</sub>/c, *a* = 18.098(2) Å, *b* = 18.151(2) Å, *c* = 12.7405-(14) Å, β = 91.62(3)°, *V* = 4183.6(8) Å<sup>3</sup>, *Z* = 4, ρ<sub>calcd</sub> = 1.357 Mg m<sup>-3</sup>; μ = 0.493 mm<sup>-1</sup>, 27 337 data (7572 unique, *R*<sub>int</sub> = 0.0510), *R* = 0.0512 for 6199 observed data, w*R*<sub>2</sub> 0.1268, *S* = 1.125 for 506 parameters. Residual electron density 1.273 and -1.090 eÅ<sup>-3</sup>. L1Pd(2,6-dipropylPy): C<sub>44</sub>H<sub>56</sub>N<sub>4</sub>O<sub>4</sub>Pd, *M<sub>r</sub>* = 811.33, yellow prism, crystal size = 0.05 × 0.03 × 0.03 mm<sup>3</sup>, monoclinic, *P*<sub>2</sub>/c, *a* = 14.437(6) Å, *b* = 18.314(6) Å, *c* = 16.522(6) Å, β = 112.17(9)°, *V* = 4045(3) Å<sup>3</sup>, *Z* = 4, ρ<sub>calcd</sub> = 1.332 Mg m<sup>-3</sup>; μ = 0.505 mm<sup>-1</sup>, 26 021 data (7361 unique *R*<sub>int</sub> = 0.2872), *R* = 0.0937 for 3061 observed data, w*R*<sub>2</sub> = 0.1982 *S* = 0.953 for 479 parameters. Residual electron density 1.263 and -0.812 eÅ<sup>-3</sup>. CCDC 651736 and 651737 contain the supplementary crystallographic data for this paper. These data can be obtained free of charge from the Cambridge Crystallographic Data Centre via www.ccdc.cam.ac.uk/data\_request/cif.

**Acknowledgment.** This work was financed by the EU project SingleMotor-FLIN and the EPSRC. We also thank the Ramsay Memorial Trust (J.D.C.), EPSRC (D.A.L.), Royal Society (P.J.L.), Deutscher Akademischer Austausch Dienst (C.P.), and the Swiss National Science Foundation (L.-E.P.-A.) for their generous support through various fellowship schemes.

**Supporting Information Available:** Experimental procedures and spectroscopic data for all new compounds, details of the model heterocycle exchange experiments, the protonation/deprotonation-driven shuttling experiments, and full crystallographic details of L1Pd(2,6-dipropylPy) and L1Pd(2,6-dipropylDMAP). This material is available free of charge via the Internet at <http://pubs.acs.org>.

JA076570H